


**Anisotropic neutron star crust, solar system mountains, and gravitational waves**J. A. Morales<sup>1,2,\*</sup> and C. J. Horowitz<sup>3,1,†</sup><sup>1</sup>*Center for the Exploration of Energy and Matter and Department of Physics,  
Indiana University, Bloomington, Indiana 47405, USA*<sup>2</sup>*Max Planck Institute for Gravitational Physics (Albert Einstein Institute),  
Callinstrasse 38, 30167 Hannover, Germany*<sup>3</sup>*Facility for Rare Isotope Beams, Michigan State University, East Lansing, Michigan 48824, USA* (Received 28 June 2023; revised 25 June 2024; accepted 9 July 2024; published 5 August 2024)

“Mountains” or nonaxisymmetric deformations of rotating neutron stars (NS) efficiently radiate gravitational waves (GW). We consider analogies between NS mountains and surface features of solar system bodies. Both NS and moons such as Europa or Enceladus have thin crusts over deep oceans while Mercury has a thin crust over a large metallic core. Thin sheets may wrinkle in universal ways. Europa has linear features, Enceladus has “tiger” stripes, and Mercury has lobate scarps. NS may have analogous features. The innermost inner core of the Earth is anisotropic with a shear modulus that depends on direction. If NS crust material is also anisotropic this will produce an ellipticity, when the crust is stressed, that grows with spin frequency. This yields a braking index (log derivative of spin down rate assuming only GW spin down) very different from  $n = 5$  and could explain the maximum spin observed for neutron stars and a possible minimum ellipticity of millisecond pulsars.

DOI: [10.1103/PhysRevD.110.044016](https://doi.org/10.1103/PhysRevD.110.044016)

The opening of the gravitational wave (GW) sky is an historic time. We have observed GW from black hole [1] and neutron star [2] mergers. Galileo opened the electromagnetic sky and its extraordinary riches. The GW sky, no doubt, contains additional very exciting signals. Galileo observed mountains on the Moon. Ongoing searches for continuous GW from “mountains” (large scale deformations) on rotating neutron stars have not yet detected signals. Targeted searches have focused on known pulsars, with known spin frequency and spin down parameters [3–22]. On the other hand, directed searches have focused on locations in the sky that are known or suspected to harbor a neutron star, without prior knowledge of neither the frequency nor any spin-down parameter [23–33]. Finally, all-sky searches have focused on searching for unknown sources at unknown locations [34–48]. These various types of searches are improving. Next generation GW observatories Cosmic Explorer and Einstein Telescope should extend these searches to hundreds to thousands of times more neutron stars [49,50].

Neutron stars, like many solar system bodies, have solid crusts. “Mountains,” or nonaxisymmetric deformations of the crust, radiate gravitational waves as the star rotates [51]. The amplitude  $h_0$  of gravitational wave radiation from a star a distance  $d$  away, rotating with rotational frequency  $\Omega$  and moment of inertia  $I$  is [52],

$$h_0 = \frac{16\pi^2 G I}{c^4} \frac{1}{d} \Omega^2 \epsilon. \quad (1)$$

Here the important unknown is the shape of the star or ellipticity  $\epsilon$  defined as the fractional difference in the star’s principle moments of inertia,

$$\epsilon = (I_1 - I_2)/I_3, \quad (2)$$

with 3 the rotation axis. Large scale deformations in the crust, or mountains, can give rise to a nonzero  $\epsilon$ .

An important first step is to calculate the maximum ellipticity that the crust can support. This involves simulating the breaking strain of neutron star crust material and then determining the maximum ellipticity the crust material can support against the star’s gravity. Molecular dynamics simulations, including the effects of impurities, defects, and grain boundaries, find that the breaking strain of the crust is large, of order 0.1, because the crust is under great pressure that prevents the formation of voids or fractures [53–55].

Given this breaking strain, the maximum ellipticity can be calculated using the intuitive formalism of Ushomirsky *et al.* [51]. They assume the crust can be strained near its breaking strain everywhere and write the maximum deformation the crust can support as a simple integral of the crust breaking stress divided by the local gravitational acceleration. This yields a maximum ellipticity  $\epsilon_{\max}$  of a few  $\times 10^{-6}$ . Note that Gittins *et al.*, using a simplified external force to deform the star, claim a smaller  $\epsilon_{\max}$  [56]. However, using Gittins *et al.*

\* Contact author: [jormal@iu.edu](mailto:jormal@iu.edu)† Contact author: [horowit@indiana.edu](mailto:horowit@indiana.edu)

formalism with an improved external force, we find a larger  $\epsilon_{\max}$  consistent with Ushmirsky *et al.* [57]. We therefore assume  $\epsilon_{\max} \approx \text{few} \times 10^{-6}$ .

This value for  $\epsilon_{\max}$  can be compared to the smallest observed upper limit, for a rapidly spinning nearby pulsar,  $\epsilon_{\min} \approx \text{few} \times 10^{-9}$  [20]. This gives a dynamic range of  $\epsilon_{\max}/\epsilon_{\min} \approx 1000$ . We can detect mountains 1000 times smaller than the maximum crust mountain.

Unfortunately, we do not know the actual size of neutron star mountains and  $\epsilon$  for particular stars. Electromagnetic observations of surface features are very limited. For example rotational phase resolved x-ray spectroscopy has mapped the shape of hot spots on some pulsars [59]. However, this thermal information does not directly provide elevations or mass distributions. Furthermore, mountain building mechanisms may be complex and depend on poorly known material properties. For example, viscoelastic creep, how a stressed elastic medium relaxes with time, may be important for the lifetime of neutron star mountains [54].

For a given postulated mechanism, for example temperature dependent electron capture on accreting stars [51], one can estimate the resulting ellipticity. However, neutron star crusts may be very rich physical systems that can involve many possible deformation mechanisms. We consider analogies between neutron star mountains and surface features of solar system bodies for two reasons. First, solar system observations may suggest particular mountain building mechanisms that could produce interesting  $\epsilon$  values for neutron stars and lead to detectable gravitational wave radiation. Second, the great diversity of solar system bodies suggests that neutron star crusts may also be diverse. Although the analogy between neutron stars and solar system bodies is incomplete, we have unique observations of solar system surface features. This provides “ground truth” for complex mountain building physics.

We consider a large range of solar system planets and moons starting from very general considerations and proceed to more specialized observations and mountain building mechanisms. Perhaps the most basic observation is that solar system moons are extraordinarily diverse. This was revealed with the first images of the Galilean moons of Jupiter from the Pioneer and Voyager spacecraft. “The satellite surfaces display dramatic differences including extensive active volcanism on Io, complex tectonism on Ganymede and possibly Europa, and flattened remnants of enormous impact features on Callisto” [60]. Not only are these four moons very different from each other, none is similar to our Moon. If neutron stars are also diverse, this could be promising for gravitational wave searches. Indeed, we know of several different classes of neutron stars such as pulsars, millisecond pulsars, or magnetars. Even if some stars are symmetric with small ellipticities, others may be very different and have larger ellipticities.

Many solar system bodies have large scale asymmetries. For example the near and far sides of the Moon are very

different. Mars is strikingly asymmetric. Not only is the low smooth northern hemisphere quite different from the high cratered southern hemisphere but great volcanoes and high plateaus make the East very different from the West [61]. Iapetus, a moon of Saturn, is extremely asymmetric with a very dark leading hemisphere and an extraordinarily bright trailing hemisphere [62]. These several bodies, with large observed asymmetries, provide at least moral support for there also being asymmetric neutron stars.

Mimas, another moon of Saturn, has a very large crater Herschel [63]. This single feature, by itself, creates a significant ellipticity. Single catastrophic events on neutron stars could likewise produce large asymmetries. For example, an event that melts a significant fraction of the crust could leave a large “scar” when the crust re-freezes and produce a nonzero ellipticity.

Leptodermous kosmos is a possible Greek translation of thin-skinned worlds. Neutron stars have a thin crust, approximately 1 km thick, over a deep liquid core. There are a number of thin-skinned moons in the solar system. Both Europa and yet another moon of Saturn Enceladus have thin ice crusts over deep oceans. These moons have characteristic linear surface features. Indeed the lines on Enceladus look like “tiger stripes.” Neutron stars, with their thin crusts, may have analogous linear surface features.

Accretion can spin up the equatorial bulge of a neutron star and put the crust under tension while EM or GW radiation can spin down the bulge and put the crust under compression. Thin sheets may wrinkle in universal ways. Examples of wrinkling under tension include hanging drapes [64], stretched thin sheets [65], or a water drop on a thin sheet [66]. Compressional examples include wrinkling from thermal contraction mismatch [67] or growth induced wrinkling in leaves and flowers [68].

The planet Mercury has a thin silicate crust over a large metallic core. Lobate scarps on Mercury are bow shaped ridges that can be hundreds of kilometers long. These are the most prominent tectonic features on the planet with a few hundred to several thousand meters of vertical relief [69–71]. The formation of these features is thought to involve the thermal contraction of the core leading to compressional wrinkling of the thin crust [72]. Neutron stars that are significantly spun down may have lobate scarp like wrinkles and these could contribute to a nonzero ellipticity.

Recent observations of seismic waves reverberating through the Earth’s center find an anisotropic innermost inner core [73]. Here the velocity of shear waves in innermost inner core material is observed to depend on direction. Don Anderson wrote, “Crystals are anisotropic and tend to be oriented by sedimentation, freezing, recrystallization, deformation, and flow. Therefore we expect the solid portions of the earth to be anisotropic to the propagation of seismic waves and material properties [74].”

We postulate that neutron star crust may also be anisotropic. This provides a new way to break axial symmetry and generate a nonzero  $\epsilon$ . Single crystals are anisotropic. Neutron star crust is believed to form a body centered cubic (bcc) lattice. A bcc lattice has a small shear modulus for compressing one axis of the lattice (and expanding the other two axis by half as much so as to conserve the volume). In addition there is an  $\approx 8$  times larger shear modulus for distorting the square lattice into a rhombus [75]. Thus a single bcc crystal has a large anisotropy and the velocity of shear waves depends strongly on direction [76].

In addition, complex nuclear pasta phases are expected over an approximately 100 m region between the crust and the core [77,78]. This region can be important because it is the densest part of the crust and may contain half of the crust's mass. Some pasta shapes, such as lasagna, are strongly anisotropic [79,80].

However, one typically assumes macroscopic regions of a neutron star involve large numbers of microcrystals (or domains) and each domain has a random orientation. As a result almost all calculations assume an angle-averaged shear modulus [81], see also [80], where the velocity of shear waves is independent of direction.

We now consider that the microcrystals may be partially aligned due to recrystallization or some other mechanism. For example, material on an accreting neutron star is constantly being both crystallized as new material is added and melted as material is buried to higher densities and dissolves into the core. This may create one or more regions, that are not negligibly small compared to the size of the star, where crystals are at least partially aligned. Each region is assumed to have a single orientation determined for example by the random orientation of a first seed crystal. Alternatively, pasta may form (partially) aligned with respect to the magnetic field with spaghetti forming along  $B$  or  $B$  in the plane of lasagna sheets [80]. The shear modulus will be anisotropic by an amount that depends on the amount of alignment of the microcrystals.

We obtain a first estimate of the ellipticity produced by an anisotropic crust with a simple two dimensional calculation. This order of magnitude result will suffice, given the large uncertainty in the anisotropy of the crust. We replace a hollow sphere by a hollow cylinder that is assumed thin in the  $z$  direction (out of the plane in Fig. 1). We consider a thin disc and treat the anisotropy as a first order perturbation to the corresponding axially symmetric constitutive relationships [82]. A thick disk is expected to yield qualitatively similar results, however the calculation is somewhat more involved.

Figure 1 shows the equatorial plane of a rotating neutron star. Elastic perturbations of the stress tensor  $\sigma_{ij}$  are related to the strain tensor  $\epsilon_{ij}$  by the elasticity of the medium,

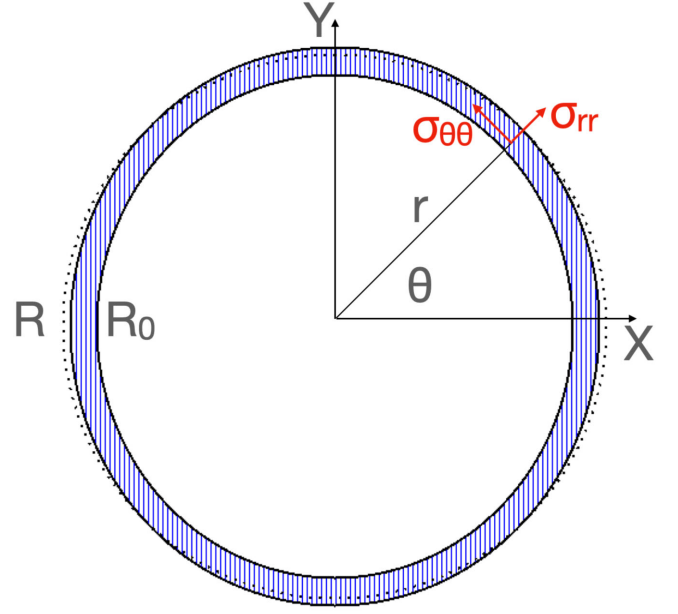


FIG. 1. Cut through the equatorial plane of a rotating star. The crust extends from  $R_0$  to  $R$  and is slightly anisotropic in the  $X$  direction.

$$\sigma_{xx} = \frac{E}{1-\nu^2} (1 + \langle \phi \rangle) \epsilon_{xx} + \frac{\nu E}{1-\nu^2} \epsilon_{yy}, \quad (3)$$

$$\sigma_{yy} = \frac{E}{1-\nu^2} \epsilon_{yy} + \frac{\nu E}{1-\nu^2} \epsilon_{xx}, \quad (4)$$

and  $\sigma_{xy} = E \epsilon_{xy} / (1 + \nu)$ , with  $E$  the Young's modulus and  $\nu$  the Poisson ratio. The degree of alignment of microcrystals in the crust is described by the small parameter  $\langle \phi \rangle$ . If  $\langle \phi \rangle = 0$  the medium is isotropic. As an example, we consider a partially aligned medium with the symmetries of the lasagna phase of nuclear pasta [80]. The  $X$  axis in Fig. 1 is normal to the lasagna planes. We assume this direction arose from spontaneous symmetry breaking, for example the random orientation of a seed microcrystal. We start with a symmetric medium  $\langle \phi \rangle = 0$  and then calculate first corrections from  $\langle \phi \rangle \neq 0$ .

We note the shear modulus is  $\mu = E/[2(1 + \nu)]$  and bulk modulus is  $K = E/[3(1 - 2\nu)]$ . We define  $\langle \phi \rangle$  to describe the degree of alignment with respect to the shear (or Young's) modulus. The larger bulk modulus (since  $\nu$  is near 0.5) may have a large contribution from the isotropic electron pressure. This symmetric pressure will tend to reduce (but not eliminate) the ellipticity of the star, see discussion of Eq. (12) below.

We assume the crust froze while the star was rotating with initial angular frequency  $\omega_0$ . If the star is then spun up or spun down to a new angular frequency  $\omega$ , stresses will be induced according to the equation of motion,

$$\frac{\partial \sigma_{rr}}{\partial r} + \frac{1}{r} (\sigma_{rr} - \sigma_{\theta\theta}) = -\rho r (\omega^2 - \omega_0^2), \quad (5)$$

with  $\rho$  the average crust density. The radial stress is [82],

$$\sigma_{rr}(r) = \frac{3+\nu}{8}\rho(\omega^2 - \omega_0^2) \left[ R^2 + R_0^2 - r^2 - \frac{R^2 R_0^2}{r^2} \right], \quad (6)$$

and satisfies boundary conditions  $\sigma_{rr}(R_0) = \sigma_{rr}(R) = 0$  at the inner  $R_0$  and outer  $R$  radii of the crust. The angular stress  $\sigma_{\theta\theta}$  is [82],

$$\sigma_{\theta\theta}(r) = \frac{3+\nu}{8}\rho(\omega^2 - \omega_0^2) \left[ R^2 + R_0^2 - \frac{1+3\nu}{3+\nu}r^2 + \frac{R^2 R_0^2}{r^2} \right], \quad (7)$$

and does not vanish at  $r = R_0$  or  $R$ .

We now consider  $\langle\phi\rangle \neq 0$ . We rewrite Eqs. (3) and (4) in polar coordinates, invert to obtain strain  $\epsilon_{ij}$  as a function of stress, and expand to lowest order in  $\langle\phi\rangle$ . We provide a first estimate of the change in strain  $\delta\epsilon_{ij}$  with  $\langle\phi\rangle$  by using the unperturbed stresses from Eqs. (6) and (7) to get,

$$\begin{bmatrix} \delta\epsilon_{rr} \\ \delta\epsilon_{\theta\theta} \end{bmatrix} \approx -\frac{\langle\phi\rangle}{E} \begin{bmatrix} \frac{(C^2 - S^2\nu)^2}{1-\nu^2} & \frac{C^2 S^2(1+\nu)}{1-\nu} \\ \frac{C^2 S^2(1+\nu)}{1-\nu} & \frac{(C^2\nu - S^2)^2}{1-\nu^2} \end{bmatrix} \begin{bmatrix} \sigma_{rr} \\ \sigma_{\theta\theta} \end{bmatrix} \quad (8)$$

with  $S = \sin\theta$  and  $C = \cos\theta$ . We assume a thin crust  $R - R_0 \ll R$  where  $\sigma_{rr} \ll \sigma_{\theta\theta}$  and  $\sigma_{\theta\theta}$  is approximately independent of  $r$ . This gives  $\delta\epsilon_{rr}$  and  $\delta\epsilon_{\theta\theta}$  that are also  $\approx$  independent of  $r$ . The radial displacement is written  $u_r = u_r^0 + \delta u_r$  where  $u_r^0$  is the displacement in the isotropic case  $\langle\phi\rangle = 0$ . Likewise  $u_\theta = u_\theta^0 + \delta u_\theta$ . The perturbation  $\delta u_r \approx (r - R_0)\delta\epsilon_{rr}(\theta)$  follows from integrating  $\partial\delta u_r/\partial r = \delta\epsilon_{rr}$ . The angular displacement follows by integrating  $\delta\epsilon_{\theta\theta} = (\partial\delta u_\theta/\partial\theta + \delta u_r)/r$  to get  $\delta u_\theta \approx \int d\theta' [r\delta\epsilon_{\theta\theta} - (r - R_0)\delta\epsilon_{rr}] + C_\theta$  or,

$$\delta u_\theta(\theta) \approx R \int_0^\theta d\theta' \delta\epsilon_{\theta\theta} + C_\theta, \quad (9)$$

assuming  $r \gg r - R_0$ . Here the integration constant  $C_\theta$  is independent of  $\theta$  and does not contribute to moments of inertia.

We now calculate the difference in moments of inertia in Eq. (2). For simplicity we work in two dimensions and actually calculate moments of inertia of a deformed hoop. This provides an order of magnitude estimate for the ellipticity. A mass  $\rho(\mathbf{r})$  that was initially at  $\mathbf{r}$  is now at  $\mathbf{r}' = (r + u_r^0 + \delta u_r)\hat{r} + (u_\theta^0 + \delta u_\theta)\hat{\theta} + u_z\hat{z}$ . The difference in moments of inertia is,

$$I_x - I_y = \int d^3r \rho(r) [(\mathbf{r}' \cdot \hat{y})^2 - (\mathbf{r}' \cdot \hat{x})^2]. \quad (10)$$

Working to first order in the small displacement  $\delta u_\theta(\theta)$ , this becomes  $I_x - I_y \approx 4 \int d^3r \rho(r) r \delta u_\theta(\theta) \sin\theta \cos\theta$ . We write

this as  $I_x - I_y \approx m_{cr} R^2 A$  where  $m_{cr} = \int d^3r \rho(r)$  is the mass of the crust and the important angular integral is

$$A = \frac{4}{2\pi} \int_0^{2\pi} d\theta \sin\theta \cos\theta \int_0^\theta d\theta' \delta\epsilon_{\theta\theta}(\theta'). \quad (11)$$

Finally, dividing by the moment of inertia  $I \approx \frac{2}{5}MR^2$ , of a star of mass  $M$ , gives the ellipticity  $\epsilon \approx \frac{5}{2} \frac{m_{cr}}{M} A$ . Using  $\sigma_{\theta\theta} \approx \rho R^2(\omega^2 - \omega_0^2)$  from Eq. (7),  $\delta\epsilon_{\theta\theta}$  from Eq. (8), and evaluating the integral gives

$$\epsilon \approx \frac{5}{16} \left( \frac{5 - 2\nu + \nu^2}{1 - \nu^2} \right) \left( \frac{m_{cr}}{M} \right) \left( \frac{\rho R^2}{E} \right) \langle\phi\rangle (\omega^2 - \omega_0^2). \quad (12)$$

This calculation has been for a thin disk where the *stress* is in the xy plane. A thick disk, where the *strain* is in the xy plane, gives a similar result. We expect results for a three dimensional sphere to also be similar. However, this should be verified in future work.

Equation (12) involves a ratio of the anisotropic stress perturbation, proportional to  $\langle\phi\rangle$ , to the isotropic stress perturbation, proportional to the Young's modulus  $E$ . In addition, there is a large isotropic stress from the pressure  $P$  that is related to the bulk modulus  $K$ . To include this, we replace  $E$  in Eq. (12) by  $3K$  [83]. Finally, we express  $3K$  in terms of the centrifugal force that balances gravity. In hydrostatic equilibrium,  $dP/dr = -GM\rho/r^2$ . The gravitational acceleration is balanced by a centrifugal acceleration  $GM/R^2 \approx \omega_K^2 R$  when the star is rotating at the Kepler or break up speed  $\omega_K$ . Therefore, we replace  $3K = -rdP/dr$  by  $\omega_K^2 R^2 \rho$  to arrive at our main result for the ellipticity of a star with anisotropic material in its crust,

$$\epsilon \approx \frac{m_{cr}}{M} \langle\phi\rangle \frac{\Omega^2 - \Omega_0^2}{\Omega_K^2}. \quad (13)$$

Note that we have rewritten the angular frequencies  $\omega$ ,  $\omega_0$ , and  $\omega_K$  in terms of rotational frequencies  $\Omega = \omega/(2\pi)$  etc. Here  $m_{cr}/M \approx 10^{-2}$  and  $\Omega_K \approx 1400$  Hz depending on the equation of state. We see that  $\epsilon$  is a strong function of the rotational frequency  $\Omega$  and the initial frequency  $\Omega_0$  (when the crust froze).

Unfortunately, we do not know the degree of anisotropy of the neutron star crust  $\langle\phi\rangle$ . Even a small average can lead to a significant  $\epsilon$  and produce observable gravitational waves. As an example we consider the innermost inner core of the Earth because we have no neutron star observations. There is a few percent anisotropy in the Earth that extends over the innermost inner core [73]. This region has a radius of 300 km and contains about  $3 \times 10^{-4}$  of the Earth's mass. If we ignore anisotropies in the rest of the Earth, this corresponds to  $\langle\phi\rangle \approx 10^{-5}$  when averaged over the Earth's total mass.

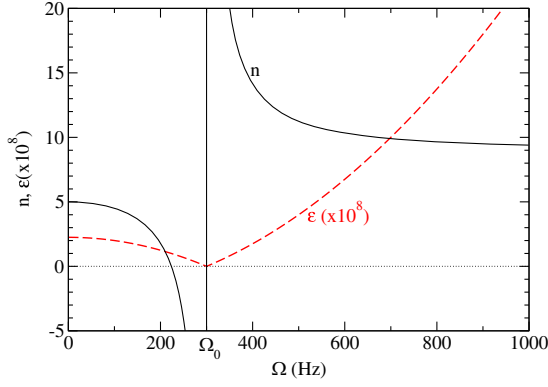


FIG. 2. Braking index  $n$  (solid black curve) and ellipticity  $\epsilon$  (dashed red curve) vs rotational frequency  $\Omega$  assuming spin down only from GW radiation and the crust froze while the star was rotating at  $\Omega_0 = 300$  Hz.

Of course this value is not directly relevant for neutron stars. Nevertheless, if material in a neutron star has an anisotropy of  $\langle\phi\rangle \approx 10^{-5}$  when averaged over the crust mass, this would yield  $\epsilon \approx 10^{-7}(\Omega^2 - \Omega_0^2)/\Omega_K^2$  or  $\epsilon \approx 10^{-8}$  for a rapidly rotating object with  $(\Omega^2 - \Omega_0^2)/\Omega_K^2 \approx 0.1$ . Gravitational waves from a nearby star could be detectable for this  $\epsilon$  value.

The braking index  $n = d \ln \dot{\omega} / d \ln \omega$  describes how the spin down rate  $\dot{\omega}$  depends on rotational frequency. For simplicity we neglect spin down from electromagnetic radiation. Spin down from gravitational wave radiation only with a frequency independent  $\epsilon$  has  $n = 5$ . However the strong spin dependence of  $\epsilon$  in Eq. (13) leads to  $n = 5 + 4\Omega^2/(\Omega^2 - \Omega_0^2)$ . This is very different from 5 as shown in Fig. 2. In the limit  $\Omega \gg \Omega_0$ ,  $n = 9$  and  $n$  changes rapidly for  $\Omega$  near  $\Omega_0$ . Neutron stars that have been spun up since crust formation have  $n > 9$  while stars that have spun down since crust formation have  $n < 5$ . Finally,  $n = 0$  at  $\Omega = \sqrt{5/9}\Omega_0$ . For constant  $\epsilon$ ,  $|\dot{\omega}|$  decreases with decreasing  $\Omega$ . However as  $\Omega$  decreases  $\epsilon$  increases (given  $\Omega < \Omega_0$ ) and this increases  $|\dot{\omega}|$ . At  $\Omega = \sqrt{5/9}\Omega_0$  the two effects cancel and  $n = 0$ .

Torque from gravitational wave radiation could balance the spin up from accretion and limit neutron star spins [51]. Using  $\epsilon$  in Eq. (13), this torque  $N_{gw}$  rises very rapidly with  $\Omega$  so  $N_{gw} \propto \Omega^5(\Omega^2 - \Omega_0^2)^2\langle\phi\rangle^2$ . If  $N_{gw}$  balances the accretion torque  $N_a \approx \dot{M}(GMR)^{1/2}$  then the equilibrium spin,

$$\Omega_{eq} \approx 300 \text{ Hz} \left( \frac{\dot{M}}{10^{-8} M_\odot \text{ yr}^{-1}} \right)^{1/9} \left( \frac{10^{-4}}{\langle\phi\rangle} \right)^{2/9}, \quad (14)$$

could agree with observed values. Note that  $\Omega_{eq}$  only depends very weakly on the accretion rate  $\dot{M}$  or  $\langle\phi\rangle$ . Here we assume  $\Omega_{eq} \gg \Omega_0$ ,  $M = 1.4M_\odot$ , and  $R \approx 10$  km. Because our ellipticity rises strongly with  $\Omega$ , this torque balance can be achieved with modest  $\langle\phi\rangle \approx 10^{-4}$ .

Furthermore, our mechanism, with a somewhat smaller  $\langle\phi\rangle \approx 10^{-5}$ , could explain a possible minimum ellipticity  $\epsilon \approx 10^{-9}$  suggested by an observed minimum spin down rate for millisecond pulsars [84].

Because the geometry of a thin disc is different from that of a realistic NS, we have performed finite-element simulations of a three-dimensional NS with a polytropic equation of state that confirm the order-of-magnitude estimate of Eq. (13). The finite-element simulations were performed using FEniCSx software with an element size of order  $10^4$  cm for a  $1.4M_\odot$  and 10 km NS [85–88]. In addition, the finite-element simulations confirm the proportionality between the ellipticity and  $\Omega^2 - \Omega_0^2$  and  $\langle\phi\rangle$ , as well as the predominance of the contribution from the azimuthal displacement  $\delta u_\theta$  to the ellipticity. The details of the finite-element simulations will be discussed in a future publication. Our simulations for an  $n = 1$  polytropic equation of state have an ellipticity

$$\epsilon \approx \frac{m_{cr}}{M} \langle\phi\rangle \frac{\Omega^2 - \Omega_0^2}{\Omega_{K,nr}^2}, \quad (15)$$

where  $\Omega_{K,nr} \approx 2200$  Hz is the rotational Kepler frequency for a Newtonian NS with an  $n = 1$  polytropic equation of state. Note that Eq. (15) is similar to Eq. (13).

In conclusion “mountains” or nonaxisymmetric deformations of rotating neutron stars (NS) efficiently radiate gravitational waves (GW). There are many ongoing searches for continuous GW from such stars. Present detectors are sensitive, in the best cases, to mountains that are 1000 times smaller than the maximum mountain that the crust can support. Unfortunately, we do not know the size of NS mountains. We consider analogies between NS mountains and surface features of solar system bodies. Here solar system observations can provide “ground truth” for complex mountain building physics. Both NS and moons such as Europa or Enceladus have thin crusts over deep oceans while Mercury has a thin crust over a large metallic core. Thin sheets may wrinkle in universal ways. Europa has linear features, Enceladus has “tiger” stripes, and Mercury has lobate scarps. NS may have analogous features. The innermost inner core of the Earth is anisotropic with a shear modulus that depends on direction. If NS crust material is also anisotropic this could produce a significant ellipticity that grows rapidly with increasing rotational frequency. Gravitational wave emission torques from this ellipticity may limit the spin rate of neutron stars.

Matt Caplan, Cole Miller, Jing Ming, and Ruedi Widmer-Schmidrig are thanked for helpful comments. This work is partially supported by the U.S. Department of Energy Grant No. DE-FG02-87ER40365 and National Science Foundation Grant No. PHY-2116686.

- [1] B. P. Abbott *et al.* (LIGO Scientific and Virgo Collaborations), Observation of gravitational waves from a binary black hole merger, *Phys. Rev. Lett.* **116**, 061102 (2016).
- [2] B. P. Abbott *et al.* (LIGO Scientific and Virgo Collaborations), GW170817: Observation of gravitational waves from a binary neutron star inspiral, *Phys. Rev. Lett.* **119**, 161101 (2017).
- [3] B. P. Abbott, R. Abbott, T. D. Abbott, S. Abraham, F. Acernese, K. Ackley, C. Adams, R. X. Adhikari, V. B. Adya, and C. Affeldt (LIGO Scientific Collaboration), Setting upper limits on the strength of periodic gravitational waves from PSR J1939 + 2134 using the first science data from the GEO 600 and LIGO detectors, *Phys. Rev. D* **69**, 082004 (2004).
- [4] B. P. Abbott, R. Abbott, T. D. Abbott, S. Abraham, F. Acernese, K. Ackley, C. Adams, R. X. Adhikari, V. B. Adya, and C. Affeldt (LIGO Scientific Collaboration), Limits on gravitational-wave emission from selected pulsars using LIGO data, *Phys. Rev. Lett.* **94**, 181103 (2005).
- [5] B. P. Abbott, R. Abbott, T. D. Abbott, S. Abraham, F. Acernese, K. Ackley, C. Adams, R. X. Adhikari, V. B. Adya, and C. Affeldt (LIGO Scientific Collaboration), Upper limits on gravitational wave emission from 78 radio pulsars, *Phys. Rev. D* **76**, 042001 (2007).
- [6] B. P. Abbott, R. Abbott, T. D. Abbott, S. Abraham, F. Acernese, K. Ackley, C. Adams, R. X. Adhikari, V. B. Adya, and C. Affeldt, Beating the spin-down limit on gravitational wave emission from the Crab pulsar, *Astrophys. J.* **683**, L45 (2008).
- [7] B. P. Abbott, R. Abbott, T. D. Abbott, S. Abraham, F. Acernese, K. Ackley, C. Adams, R. X. Adhikari, V. B. Adya, and C. Affeldt, Searches for gravitational waves from unknown pulsar with science run 5 LIGO data, *Astrophys. J.* **713**, 671 (2010).
- [8] J. Abadie *et al.* (The LIGO Scientific Collaboration), Search for gravitational waves associated with the August 2006 timing glitch of the Vela pulsar, *Phys. Rev. D* **83**, 042001 (2011).
- [9] J. Abadie *et al.*, Beating the spin-down limit on gravitational wave emission from the Vela pulsar, *Astrophys. J.* **737**, 93 (2011).
- [10] J. Aasi *et al.*, Gravitational waves from known pulsars: Results from the initial detector era, *Astrophys. J.* **785**, 119 (2014).
- [11] J. Aasi, B. P. Abbott, R. Abbott, T. D. Abbott, S. Abraham, F. Acernese, K. Ackley, C. Adams, R. X. Adhikari, V. B. Adya, and C. Affeldt (LIGO Scientific and Virgo Collaborations), Narrow-band search of continuous gravitational-wave signals from Crab and Vela pulsars in Virgo VSR4 data, *Phys. Rev. D* **91**, 022004 (2015).
- [12] J. Aasi, B. P. Abbott, R. Abbott, T. D. Abbott, S. Abraham, F. Acernese, K. Ackley, C. Adams, R. X. Adhikari, V. B. Adya, and C. Affeldt (LIGO Scientific and Virgo Collaborations), Directed search for gravitational waves from Scorpius X-1 with initial LIGO data, *Phys. Rev. D* **91**, 062008 (2015).
- [13] B. P. Abbott, R. Abbott, T. D. Abbott, S. Abraham, F. Acernese, K. Ackley, C. Adams, R. X. Adhikari, V. B. Adya, and C. Affeldt, First search for gravitational waves from known pulsars with Advanced LIGO, *Astrophys. J.* **839**, 12 (2017).
- [14] B. P. Abbott, R. Abbott, T. D. Abbott, S. Abraham, F. Acernese, K. Ackley, C. Adams, R. X. Adhikari, V. B. Adya, and C. Affeldt (LIGO Scientific and Virgo Collaborations), First narrow-band search for continuous gravitational waves from known pulsars in advanced detector data, *Phys. Rev. D* **96**, 122006 (2017).
- [15] B. P. Abbott, R. Abbott, T. D. Abbott, S. Abraham, F. Acernese, K. Ackley, C. Adams, R. X. Adhikari, V. B. Adya, and C. Affeldt (LIGO Scientific and Virgo Collaborations), First search for nontensorial gravitational waves from known pulsars, *Phys. Rev. Lett.* **120**, 031104 (2018).
- [16] B. P. Abbott, R. Abbott, T. D. Abbott, S. Abraham, F. Acernese, K. Ackley, C. Adams, R. X. Adhikari, V. B. Adya, and C. Affeldt (LIGO Scientific and Virgo Collaborations), Narrow-band search for gravitational waves from known pulsars using the second LIGO observing run, *Phys. Rev. D* **99**, 122002 (2019).
- [17] B. P. Abbott, R. Abbott, T. D. Abbott, S. Abraham, F. Acernese, K. Ackley, C. Adams, R. X. Adhikari, V. B. Adya, and C. Affeldt, Searches for gravitational waves from known pulsars at two harmonics in 2015–2017 LIGO data, *Astrophys. J.* **879**, 10 (2019).
- [18] A. Ashok, B. Beheshtipour, M. A. Papa, P. C. C. Freire, B. Steltner, B. Machenschalk, O. Behnke, B. Allen, and R. Prix, New searches for continuous gravitational waves from seven fast pulsars, *Astrophys. J.* **923**, 85 (2021).
- [19] B. Rajbhandari, B. J. Owen, S. Caride, and R. Inta, First searches for gravitational waves from  $r$ -modes of the Crab pulsar, *Phys. Rev. D* **104**, 122008 (2021).
- [20] R. Abbott, H. Abe, F. Acernese, K. Ackley, N. Adhikari, R. X. Adhikari, V. K. Adkins, and V. B. Adya, Searches for gravitational waves from known pulsars at two harmonics in the second and third LIGO-Virgo observing runs, *Astrophys. J.* **935**, 1 (2022).
- [21] R. Abbott, T. D. Abbott, F. Acernese, K. Ackley, C. Adams, N. Adhikari, R. X. Adhikari, and V. B. Adya, Narrowband searches for continuous and long-duration transient gravitational waves from known pulsars in the LIGO-Virgo third observing run, *Astrophys. J.* **932**, 133 (2022).
- [22] R. Abbott, T. D. Abbott, F. Acernese, K. Ackley, C. Adams, N. Adhikari, R. X. Adhikari, and V. B. Adya (LIGO Scientific, Virgo, and KAGRA Collaborations), Search for continuous gravitational waves from 20 accreting millisecond x-ray pulsars in O3 LIGO data, *Phys. Rev. D* **105**, 022002 (2022).
- [23] B. P. Abbott, R. Abbott, T. D. Abbott, S. Abraham, F. Acernese, K. Ackley, C. Adams, R. X. Adhikari, V. B. Adya, and C. Affeldt (LIGO Scientific and Virgo Collaborations), Search for gravitational waves from Scorpius X-1 in the first Advanced LIGO observing run with a hidden Markov model, *Phys. Rev. D* **95**, 122003 (2017).
- [24] B. P. Abbott, R. Abbott, T. D. Abbott, S. Abraham, F. Acernese, K. Ackley, C. Adams, R. X. Adhikari, V. B. Adya, and C. Affeldt, Upper limits on gravitational waves from Scorpius X-1 from a model-based cross-correlation search in Advanced LIGO data, *Astrophys. J.* **847**, 47 (2017).
- [25] B. P. Abbott, R. Abbott, T. D. Abbott, S. Abraham, F. Acernese, K. Ackley, C. Adams, R. X. Adhikari, V. B. Adya, and C. Affeldt (LIGO Scientific and Virgo Collaborations), Search for gravitational waves from Scorpius X-1 in

- the second Advanced LIGO observing run with an improved hidden Markov model, *Phys. Rev. D* **100**, 122002 (2019).
- [26] V. Dergachev, M. A. Papa, B. Steltner, and H.-B. Eggenstein, Loosely coherent search in LIGO O1 data for continuous gravitational waves from Terzan 5 and the galactic center, *Phys. Rev. D* **99**, 084048 (2019).
- [27] J. Ming, M. A. Papa, A. Singh, H.-B. Eggenstein, S. J. Zhu, V. Dergachev, Y. Hu, R. Prix, B. Machenschalk, C. Beer, O. Behnke, and B. Allen, Results from an Einstein@Home search for continuous gravitational waves from Cassiopeia A, Vela Jr., and G347.3, *Phys. Rev. D* **100**, 024063 (2019).
- [28] O. J. Piccinni, P. Astone, S. D'Antonio, S. Frasca, G. Intini, I. La Rosa, P. Leaci, S. Mastrogiovanni, A. Miller, and C. Palomba, Directed search for continuous gravitational-wave signals from the galactic center in the Advanced LIGO second observing run, *Phys. Rev. D* **101**, 082004 (2020).
- [29] M. Millhouse, L. Strang, and A. Melatos, Search for gravitational waves from 12 young supernova remnants with a hidden Markov model in Advanced LIGO's second observing run, *Phys. Rev. D* **102**, 083025 (2020).
- [30] L. Lindblom and B. J. Owen, Directed searches for continuous gravitational waves from twelve supernova remnants in data from Advanced LIGO's second observing run, *Phys. Rev. D* **101**, 083023 (2020).
- [31] Y. Zhang, M. A. Papa, B. Krishnan, and A. L. Watts, Search for continuous gravitational waves from Scorpius X-1 in LIGO O2 data, *Astrophys. J. Lett.* **906**, L14 (2021).
- [32] J. Ming, M. A. Papa, H.-B. Eggenstein, B. Machenschalk, B. Steltner, R. Prix, B. Allen, and O. Behnke, Results from an Einstein@Home search for continuous gravitational waves from G347.3 at low frequencies in LIGO O2 data, *Astrophys. J.* **925**, 8 (2022).
- [33] B. J. Owen, L. Lindblom, and L. S. Pinheiro, First constraining upper limits on gravitational-wave emission from NS 1987a in SNR 1987a, *Astrophys. J. Lett.* **935**, L7 (2022).
- [34] B. P. Abbott, R. Abbott, T. D. Abbott, S. Abraham, F. Acernese, K. Ackley, C. Adams, R. X. Adhikari, V. B. Adya, and C. Affeldt (LIGO Scientific Collaboration), First all-sky upper limits from LIGO on the strength of periodic gravitational waves using the Hough transform, *Phys. Rev. D* **72**, 102004 (2005).
- [35] B. P. Abbott, R. Abbott, T. D. Abbott, S. Abraham, F. Acernese, K. Ackley, C. Adams, R. X. Adhikari, V. B. Adya, and C. Affeldt (LIGO Scientific Collaboration), Searches for periodic gravitational waves from unknown isolated sources and Scorpius X-1: Results from the second LIGO science run, *Phys. Rev. D* **76**, 082001 (2007).
- [36] B. P. Abbott, R. Abbott, T. D. Abbott, S. Abraham, F. Acernese, K. Ackley, C. Adams, R. X. Adhikari, V. B. Adya, and C. Affeldt (LIGO Scientific Collaboration), All-sky search for periodic gravitational waves in LIGO S4 data, *Phys. Rev. D* **77**, 022001 (2008).
- [37] B. P. Abbott, R. Abbott, T. D. Abbott, S. Abraham, F. Acernese, K. Ackley, C. Adams, R. X. Adhikari, V. B. Adya, and C. Affeldt (LIGO Scientific Collaboration), Einstein@Home search for periodic gravitational waves in LIGO S4 data, *Phys. Rev. D* **79**, 022001 (2009).
- [38] J. Abadie *et al.* (The LIGO Scientific and The Virgo Collaborations), All-sky search for periodic gravitational waves in the full S5 LIGO data, *Phys. Rev. D* **85**, 022001 (2012).
- [39] J. Aasi, B. P. Abbott, R. Abbott, T. D. Abbott, S. Abraham, F. Acernese, K. Ackley, C. Adams, R. X. Adhikari, V. B. Adya, and C. Affeldt (The LIGO Scientific and the Virgo Collaborations), Einstein@Home all-sky search for periodic gravitational waves in LIGO S5 data, *Phys. Rev. D* **87**, 042001 (2013).
- [40] B. P. Abbott, R. Abbott, T. D. Abbott, S. Abraham, F. Acernese, K. Ackley, C. Adams, R. X. Adhikari, V. B. Adya, and C. Affeldt (LIGO Scientific and Virgo Collaborations), Comprehensive all-sky search for periodic gravitational waves in the sixth science run LIGO data, *Phys. Rev. D* **94**, 042002 (2016).
- [41] B. P. Abbott, R. Abbott, T. D. Abbott, S. Abraham, F. Acernese, K. Ackley, C. Adams, R. X. Adhikari, V. B. Adya, and C. Affeldt (LIGO Scientific and Virgo Collaborations), All-sky search for periodic gravitational waves in the O1 LIGO data, *Phys. Rev. D* **96**, 062002 (2017).
- [42] B. P. Abbott, R. Abbott, T. D. Abbott, S. Abraham, F. Acernese, K. Ackley, C. Adams, R. X. Adhikari, V. B. Adya, and C. Affeldt (LIGO Scientific and Virgo Collaborations), Full band all-sky search for periodic gravitational waves in the O1 LIGO data, *Phys. Rev. D* **97**, 102003 (2018).
- [43] V. Dergachev and M. Papa, Results from the first all-sky search for continuous gravitational waves from small-ellipticity sources, *Phys. Rev. Lett.* **125**, 171101 (2020).
- [44] V. Dergachev and M. A. Papa, Search for continuous gravitational waves from small-ellipticity sources at low frequencies, *Phys. Rev. D* **104**, 043003 (2021).
- [45] P. B. Covas, M. A. Papa, R. Prix, and B. J. Owen, Constraints on r-modes and mountains on millisecond neutron stars in binary systems, *Astrophys. J. Lett.* **929**, L19 (2022).
- [46] R. Abbott, H. Abe, F. Acernese, K. Ackley, N. Adhikari, R. X. Adhikari, V. K. Adkins, and V. B. Adya (LIGO Scientific, Virgo, and KAGRA Collaborations), All-sky search for continuous gravitational waves from isolated neutron stars using Advanced LIGO and Advanced Virgo O3 data, *Phys. Rev. D* **106**, 102008 (2022).
- [47] V. Dergachev and M. A. Papa, A frequency resolved atlas of the sky in continuous gravitational waves, *Phys. Rev. X* **13**, 021020 (2023).
- [48] B. Steltner, M. A. Papa, H.-B. Eggenstein, R. Prix, M. Bensch, B. Allen, and B. Machenschalk, Deep Einstein@Home all-sky search for continuous gravitational waves in LIGO O3 public data, *Astrophys. J.* **952**, 55 (2023).
- [49] B. Reed, A. Deibel, and C. Horowitz, Modelling the galactic neutron star population for use in continuous gravitational-wave searches, *Astrophys. J.* **921**, 89 (2021).
- [50] G. Pagliaro, M. A. Papa, J. Ming, J. Lian, D. Tsuna, C. Maraston, and D. Thomas, Continuous gravitational waves from galactic neutron stars: Demography, detectability and prospects, *Astrophys. J.* **952**, 123 (2023).
- [51] G. Ushomirsky, C. Cutler, and L. Bildsten, Deformations of accreting neutron star crusts and gravitational wave emission, *Mon. Not. R. Astron. Soc.* **319**, 902 (2000).
- [52] K. Riles, Searches for continuous-wave gravitational radiation, *Living Rev. Relativity* **26**, 3 (2023).

- [53] C. Horowitz and K. Kadau, Breaking strain of neutron star crust and gravitational waves, *Phys. Rev. Lett.* **102**, 191102 (2009).
- [54] A. I. Chugunov and C. J. Horowitz, Breaking stress of neutron star crust, *Mon. Not. R. Astron. Soc.* **407**, L54 (2010).
- [55] M. Caplan, A. Schneider, and C. Horowitz, Elasticity of nuclear pasta, *Phys. Rev. Lett.* **121**, 132701 (2018).
- [56] F. Gittins, N. Andersson, and D. Jones, Modelling neutron star mountains, *Mon. Not. R. Astron. Soc.* **500**, 5570 (2021).
- [57] J. A. Morales and C. J. Horowitz, Neutron star crust can support a large ellipticity, *Mon. Not. R. Astron. Soc.* **517**, 5610 (2022).
- [58] R. Abbott *et al.*, Searches for gravitational waves from known pulsars at two harmonics in the second and third LIGO-Virgo observing runs, *Astrophys. J.* **935**, 1 (2022).
- [59] M. C. Miller *et al.*, PSR J0030 + 0451 mass and radius from NICER data and implications for the properties of neutron star matter, *Astrophys. J. Lett.* **887**, L24 (2019).
- [60] B. A. Smith *et al.*, The Jupiter system through the eyes of Voyager 1, *Science* **204**, 951 (1979).
- [61] S. C. Solomon, O. Aharonson, J. M. Aurnou, W. B. Banerdt, M. H. Carr, A. J. Dombard, H. V. Frey, M. P. Golombek, S. A. Hauck, J. W. Head, B. M. Jakosky, C. L. Johnson, P. J. McGovern, G. A. Neumann, R. J. Phillips, D. E. Smith, and M. T. Zuber, New perspectives on ancient Mars, *Science* **307**, 1214 (2005).
- [62] S. W. Squyres and C. Sagan, Albedo asymmetry of Iapetus, *Nature (London)* **303**, 782 (1983).
- [63] S. J. Robbins, J. D. Riggs, and A. H. Parker, Is the diameter of Herschel crater, Mimas, an outlier? a mathematical framework for analyzing planetary feature size-frequency distribution anomalies, *Geophys. Res. Lett.* **48**, e2021GL093247 (2021).
- [64] H. Vandeparre, M. Piñeira, F. Brau, B. Roman, J. Bico, C. Gay, W. Bao, C. N. Lau, P. M. Reis, and P. Damman, Wrinkling hierarchy in constrained thin sheets from suspended graphene to curtains, *Phys. Rev. Lett.* **106**, 224301 (2011).
- [65] E. Cerda and L. Mahadevan, Geometry and physics of wrinkling, *Phys. Rev. Lett.* **90**, 074302 (2003).
- [66] J. Huang, M. Juskiewicz, W. H. de Jeu, E. Cerda, T. Emrick, N. Menon, and T. P. Russell, Capillary wrinkling of floating thin polymer films, *Science* **317**, 650 (2007).
- [67] B.-K. Lai, K. Kerman, and S. Ramanathan, On the role of ultra-thin oxide cathode synthesis on the functionality of microsolid oxide fuel cells: Structure, stress engineering and *in situ* observation of fuel cell membranes during operation, *J. Power Sources* **195**, 5185 (2010).
- [68] B. Audoly and A. Boudaoud, Self-similar structures near boundaries in strained systems, *Phys. Rev. Lett.* **91**, 086105 (2003).
- [69] R. G. Strom, N. J. Trask, and J. E. Guest, Tectonism and volcanism on mercury, *J. Geophys. Res.* (1896–1977) **80**, 2478 (1975).
- [70] T. R. Watters, M. S. Robinson, and A. C. Cook, Topography of lobate scarps on Mercury: New constraints on the planet's contraction, *Geology* **26**, 991 (1998).
- [71] S. C. Solomon, The relationship between crustal tectonics and internal evolution in the Moon and Mercury, *Phys. Earth Planet. Interiors* **15**, 135 (1977).
- [72] S. D. King, Pattern of lobate scarps on Mercury's surface reproduced by a model of mantle convection, *Nat. Geosci.* **1**, 229 (2008).
- [73] T.-S. Pham and H. Tkalčić, Up-to-fivefold reverberating waves through the Earth's center and distinctly anisotropic innermost inner core, *Nat. Commun.* **14**, 754 (2023).
- [74] D. L. Anderson, The inner inner core of earth, *Proc. Natl. Acad. Sci. U.S.A.* **99**, 13966 (2002).
- [75] C. J. Horowitz and J. Hughto, Molecular dynamics simulation of shear moduli for Coulomb crystals, [arXiv:0812.2650](https://arxiv.org/abs/0812.2650).
- [76] T. Tsang and H.-Y. Park, Sound velocity anisotropy in cubic crystals, *Phys. Lett.* **99A**, 377 (1983).
- [77] D. G. Ravenhall, C. J. Pethick, and J. R. Wilson, Structure of matter below nuclear saturation density, *Phys. Rev. Lett.* **50**, 2066 (1983).
- [78] M. E. Caplan and C. J. Horowitz, Colloquium: Astromaterial science and nuclear pasta, *Rev. Mod. Phys.* **89**, 041002 (2017).
- [79] C. Pethick and A. Potekhin, Liquid crystals in the mantles of neutron stars, *Phys. Lett. B* **427**, 7 (1998).
- [80] C. J. Pethick, Z.-W. Zhang, and D. N. Kobyakov, Elastic properties of phases with nonspherical nuclei in dense matter, *Phys. Rev. C* **101**, 055802 (2020).
- [81] D. N. Blaschke, Averaging of elastic constants for polycrystals, *J. Appl. Phys.* **122**, 145110 (2017).
- [82] P. Kelly, *Solid Mechanics Lecture Notes* (The University of Auckland, Auckland, 2013).
- [83] For a nearly spherical system  $-rdP/dr = -3VdP/dV = 3K$  for a system of volume  $V$ .
- [84] G. Woan, M. D. Pitkin, B. Haskell, D. I. Jones, and P. D. Lasky, Evidence for a minimum ellipticity in millisecond pulsars, *Astrophys. J. Lett.* **863**, L40 (2018).
- [85] I. A. Baratta, J. P. Dean, J. S. Dokken, M. Habera, J. S. Hale, C. N. Richardson, M. E. Rognes, M. W. Scroggs, N. Sime, and G. N. Wells, DOLFINx: The next generation FEniCS problem solving environment, preprint (2023), [10.5281/zenodo.10447666](https://zenodo.org/record/10447666).
- [86] M. W. Scroggs, I. A. Baratta, C. N. Richardson, and G. N. Wells, Basix: A runtime finite element basis evaluation library, *J. Open Source Software* **7**, 3982 (2022).
- [87] M. W. Scroggs, J. S. Dokken, C. N. Richardson, and G. N. Wells, Construction of arbitrary order finite element degree-of-freedom maps on polygonal and polyhedral cell meshes, *ACM Trans. Math. Softw.* **48**, 1 (2022).
- [88] M. S. Alnaes, A. Logg, K. B. Ølgaard, M. E. Rognes, and G. N. Wells, Unified form language: A domain-specific language for weak formulations of partial differential equations, *ACM Trans. Math. Softw.* **40**, 1 (2014).